K0423), and the National Health Institute (HL-37351 and HL-21001). S.L.G. would like to thank the American Heart Association—Wisconsin Affiliate—for providing fellowship support.

References and Notes

(1) Cooper, S. L.; Tobolsky, A. V. *J. Appl. Polym. Sci.* **1966**, *10*, 1837.
(2) Allport, D. C., Janes, W. H., Eds. *Block Copolymers*; Wiley: New York, 1973.
(3) Estes, G. M.; Cooper, S. L. *Macromolecules* **1971**, *4*, 452.
(4) Seymour, R. W.; Cooper, S. L. *Rubber Chem. Technol.* **1974**, *47*, 19.
(5) Brunette, C. M.; Hsu, S. L.; Rossman, M.; MacKnight, W. J.; Scheider, N. S. *Polym. Eng. Sci.* **1981**, *21*, 668.
(6) Gibson, P. E.; Vallance, M. A.; Cooper, S. L. In *Developments in Block Copolymers-1*; Goodman, I., Ed.; Applied Science: London, 1982.
(7) Fridman, I. D.; Thomas, E. L. *Polymer* **1980**, *21*, 388.
(8) Bonart, R. *J. Macromol. Sci., Phys.* **1968**, *B2*, 1, 115.
(9) Clough, S. B.; Schneider, N. S.; King, A. O. *J. Macromol Sci., Phys.* **1968**, *B2*, 641.
(10) Samuels, S. L.; Wilkes, G. L. *J. Polym. Sci. Symp.* **1973**, *43*, 149.
(11) Schneider, N. S.; Desper, C. R.; Illinger, J. L.; King, A. O.; Barr, D. *J. Macromol Sci., Phys.* **1975**, *B11*, 5.
(12) Van Bogart, J. W. C. Ph.D. Thesis, University of Wisconsin, 1981.
(13) Speckhard, T. A.; Ver Strate, G.; Gibson, P. E.; Cooper, S. L. *Polym. Eng. Sci.* **1983**, *23*, 337.
(14) Chang, Y. J. P.; Wilkes, G. L. *J. Polym. Sci., Polym. Phys. Ed.* **1975**, *13*, 455.
(15) Hesketh, T. R.; Van Bogart, J. W. C.; Cooper, S. L. *Polym. Eng. Sci.* **1980**, *20*, 3, 190.
(16) Lagasse, R. R. *J. Appl. Polym. Sci.* **1977**, *21*, 2489.
(17) Chang, A. L.; Thomas, E. L. In *Multiphase Polymers*; Cooper, S. L., Estes, G. M., Eds.; American Chemical Society: Washington, DC, 1979. Briber, R. M.; Thomas, E. L. *J. Macromol. Sci., Phys.* **1983**, *B22*, 509.
(18) Wilkes, G. L.; Samuels, S. L.; Crystal, R. *J. Macromol. Sci., Phys.* **1974**, *B10*, 203.
(19) Koutsky, J. A.; Hein, N. V.; Cooper, S. L. *J. Polym. Sci., Polym. Lett. Ed.* **1970**, *8*, 353.
(20) Cowie, J. M. G. In *Developments in Block Copolymers*; Goodman, I., Ed.; Applied Science: London, 1982.
(21) Roche, E. J.; Thomas, E. L. *Polymer* **1981**, *22*, 333.
(22) Handlin, D. L.; MacKnight, W. J.; Thomas, E. L. *Macromolecules* **1980**, *14*, 795.
(23) Kato, K. *Polym. Eng. Sci.* **1967**, *7*, 38.
(24) Galeski, A.; Argon, A. S.; Cohen, R. E. *Makromol. Chem.*, submitted for publication.
(25) Pawley, J. B. *Ultramicroscopy* **1984**, *13*, 387.
(26) Berry, V. K. *Proc. EMSA* **1987**, 468.
(27) Foks, J.; Michler, G. *J. Appl. Polym. Sci.* **1986**, *31*, 1281.
(28) Pawley, J. B.; Scala, W. R. *Proc. EMSA* **1986**, 654.
(29) Chen, C. H. Y.; Briber, R. M.; Thomas, E. L.; Xu, M.; MacKnight, W. J. *Polymer* **1983**, *24*, 1333.
(30) Chen-Tsai, C. H. Y.; Thomas, E. L.; MacKnight, W. J.; Schneider, N. S. *Polymer* **1986**, *27*, 659.
(31) Serrano, M.; Ottino, J. M.; Thomas, E. L.; MacKnight, W. J. *Polymer* **1987**, *28*, 1667.
(32) Ogata, S.; Maeda, H.; Kakimoto, M.; Imai, Y. *J. Appl. Polym. Sci.* **1987**, *33*, 775.
(33) Goodman, S. L.; Li, C.; Albrecht, R. M.; Cooper, S. L. *Abstr. 61st Colloid Surf. Sci. Symp.* **1987**, 220.
(34) Cullity, B. D. *Elements of X-Ray Diffraction*, 2nd ed.; Addison-Wesley: Reading, 1978; pp 127–131.
(35) Li, C.; Cooper, S. L. *Bull. Am. Phys. Soc.* **1987**, *32*, 664.
(36) Dieterich, D. In *Polyurethane Handbook*; Oertel, G., Ed.; Hansen: New York, 1985; pp 19–22.
(37) Hepburn, C. *Polyurethane Elastomers*; Applied Science: New York, 1982; Chapter 2, pp 27–48.
(38) Goodman, S. L.; Albrecht, R. M. *Scanning Microsc.* **1987**, *1*, 727.
(39) Pawley, J. B. *Proc. EMSA* **1987**, 550.
(40) Kinning, D. J.; Thomas, E. L. *Macromolecules* **1984**, *17*, 1712.
(41) Hasegawa, T.; Hashimoto, T. *Macromolecules* **1985**, *18*, 589.
(42) Kinning, D. J.; Thomas, E. L.; Ottino, J. L. *Macromolecules* **1987**, *20*, 1129.
(43) Goodman, S. L.; Li, C.; Pawley, J. B.; Cooper, S. L.; Albrecht, R. M. In *Progress in Biomedical Engineering*; Ratner, B. D., Ed.; Elsevier: Amsterdam, 1988; in press.

Crystal Structure and Morphology of Syndiotactic Polypropylene Single Crystals

Bernard Lotz,*[1] Andrew J. Lovinger,* and Rudolf E. Cais

AT&T Bell Laboratories, Murray Hill, New Jersey 07974. *Received October 23, 1987*

ABSTRACT: Large, highly regular single crystals of syndiotactic polypropylene (sPP), grown for the first time and examined by electron microscopy and electron diffraction, reveal extra reflections and characteristic streaks that had not been reported in the published X-ray fiber structure analysis of Corradini, Natta, et al.[2] On the basis of these findings, we propose that the unit cell in these crystals is orthorhombic with a = 14.50 Å, b = 11.20 Å, c = 7.40 Å, space group *Ibca*; this unit cell has a strong subcell with b = 5.60 Å. The new cell symmetry results from the presence of *both* left- *and* right-handed helices, while the earlier unit cell[2] (having the $C222_1$ space group) is based upon helices that are *all* of the *same* hand. We show that in actual crystals both packing schemes coexist leading to intermolecular-lattice disorder and thereby to the observed streaking during electron diffraction. The habit of sPP single crystals is rectangular with the b axis of the unit cell parallel to the long dimension of the crystals.

Introduction

The crystal structure and morphology of syndiotactic polypropylene (sPP) have been investigated less than those of its isotactic counterpart (iPP). Corradini et al.[2] reported the crystal structure and molecular conformation of sPP in 1967. The molecular conformation is unusual in that the sequence of rotation angles *ggttggtt* implies that successive CH_2 groups have significantly different environments, a feature amply confirmed by NMR investigations.[3] The proposed unit cell[2] is orthorhombic with parameters a = 14.50 Å, b = 5.60 Å, c (fiber axis) = 7.40 Å, and space group $C222_1$; this space group preserves in the lattice all the symmetry elements of the polymer chains. Single crystals of sPP, grown from a variety of solvents by Marchetti and Martuscelli,[4] were elongated, but their lifetimes under the electron beam were reportedly too short to enable a diffraction investigation, so that the structure-morphology relationship could not be established unequivocally.

We report in this paper an electron microscopic and electron diffraction investigation of single crystals of sPP produced by thin-film growth. The diffraction patterns

0024-9297/88/2221-2375$01.50/0

of these crystals display several features that had not been exhibited in the fiber patterns of Corradini et al.[2] These make it necessary to reexamine the structure of crystalline syndiotactic polypropylene, specifically the chain packing. In light of the results presented in this paper, the unit cell and chain packing in the literature[2] will turn out to be a special case within a range of possible packings.

Experimental Section

Materials. Single crystals of syndiotactic polypropylene were first observed admixed with a majority of isotactic polypropylene crystals in thin films of a sample of nominally atactic polypropylene, A-fax 500 (manufactured by Hercules, Inc.), a material which is known to have a low isotactic triad content. However, the main specimens used in this investigation were samples of sPP synthesized and purified in our laboratory as described below.

Synthesis. Syndiotactic polypropylene was prepared with a homogeneous vanadium-based catalyst system according to the procedure described by Boor and Youngman.[5] The solvent of choice was heptane, owing to the enhanced syndiotactic fraction formed in this medium, even though toluene gives an improved yield.[6] Heptane was supplied by Burdick and Jackson Laboratories as the distilled-in-glass grade. It was stirred over concentrated sulfuric acid, washed with water, passed through a column of neutral alumina, refluxed over sodium, and distilled. Propylene (Matheson Gas Co., CP grade, 99% purity) was subject to repeated freeze–pump–thaw cycles under vacuum to remove air and stirred with diethylaluminum chloride before being distilled. Vanadium tetrachloride (Alfa Products, Morton Thiokol, Inc.) was degassed and distilled under vacuum. Anisole (Aldrich Chemical Co.) was dried with calcium hydride and distilled. A 25% w/w solution of diisobutylaluminum chloride in hexane (95% active Al) was obtained from Alfa Products and used as received.

The catalyst solution was prepared under dry nitrogen by mixing 4 mmol of anisole with 4 mmol of vanadium tetrachloride in 400 mL of heptane at room temperature. The solution was then cooled to −78 °C, and all subsequent additions were performed at this temperature. Next, 20 mmol of diisobutylaluminum chloride at −78 °C was added to form a dark purple solution of the active catalyst, followed immediately by the final addition of 2.4 mol of propylene, so that there was no appreciable aging of the catalyst. Polymerization commenced immediately and was allowed to proceed for 3.5 h at −78 °C without stirring, after which the reaction was quenched by the addition of a large excess of methanol. The yield of polymer was only 0.16% by weight, and the polymer was dissolved in 1,2,4-trichlorobenzene, reprecipitated in methanol, and dried under vacuum for 18 h.

The tacticity of the polymer was measured by carbon-13 NMR on a Varian XL-200 spectrometer operating at 50.3 MHz. The polymer was dissolved in 1,2,4-trichlorobenzene (5% w/v) and observed at 120 °C with broadband and proton decoupling. A total of 14 000 transients was accumulated with an 8000-Hz sweep width, 32K data points, and a 90° (18 μs) pulse. The polymer contained a trace amount of head-to-head, tail-to-tail regioirregular defects as monitored by the methyl carbon resonances.[7] The main head-to-tail methyl resonances are shown in Figure 1 with all ten pentad stereosequence assignments.[8] The racemic dyad content is 76.9%, with a significant deviation from simple Bernoullian statistics. The observed triad probabilities are *mm* 0.159, *mr* 0.143, and *rr* 0.698, which may be compared with the corresponding values of 0.053, 0.355, and 0.591, respectively, for a Bernoullian distribution. The conventional interpretation of this analysis is that the polymer appears to be stereoblock, with predominantly syndiotactic sequences and a smaller fraction of isotactic sequences.

Methods. Thin films of the polymers were prepared on cleaved mica or on glass microscope cover slides by evaporation from a semidilute solution, usually in trichlorobenzene. Thermal treatments included melting at ~170 °C and slow cooling (0.2 °C/min) in a Mettler microscope heating stage under a film of dried nitrogen. The samples were subjected to conventional Pt–C shadowing and carbon backing. Examination was performed at 80 or 100 keV using a JEOL 100-CX electron microscope. Nonequatorial sections of reciprocal space were explored by use of tilting and rotating electron-microscope stages. The features described here were found in both monolayer and multilayer crystals (in film thicknesses up to 0.1 μm) and therefore do not result from influences of the substrate or from ultrathin film effects.

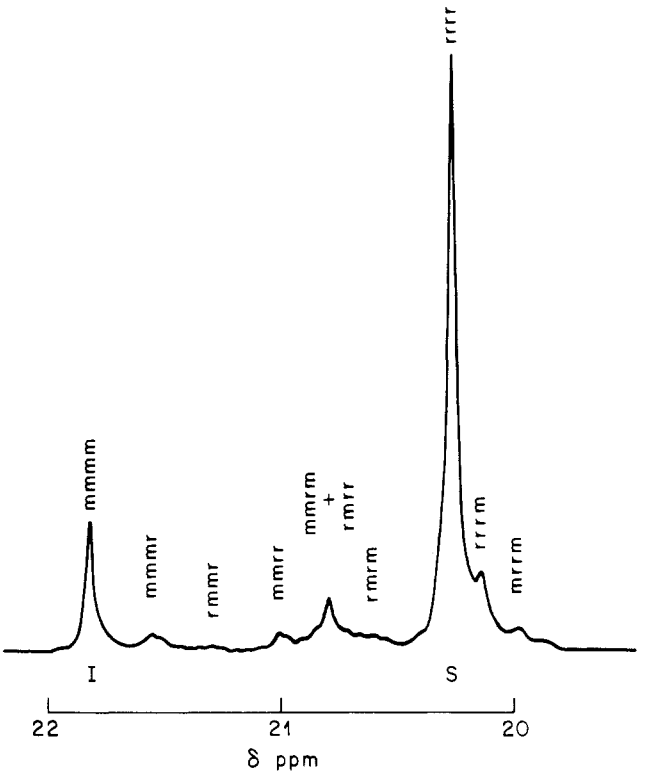

Figure 1. Expansion of the 50.3-Hz methyl carbon-13 NMR signal from polypropylene prepared with a syndiospecific catalyst, showing the main syndiotactic peak S and the isotactic fraction I. The syndiotactic dyad probability is $p(r) = 0.769$. The stereochemical pentad assignments indicated on the figure are taken from ref 8.

Results and Discussion

1. Crystal Morphology. The crystal morphology of syndiotactic polypropylene varies to some extent with crystallization conditions. As indicated by Marchetti and Martuscelli,[4] single crystals grown from solution are narrow and elongated, with ill-defined end facets (Figure 2a). On the other hand, our crystals grown from thin films in the melt are much larger and have a regular rectangular habit with slightly irregular end facets (Figure 2b,c). Electron-diffraction patterns (discussed in detail below) show that the crystallographic *b* axis is parallel to the long axis of the crystals (both those grown from solution and from the melt), whose lateral faces are therefore the densely packed (100).

2. Electron-Diffraction Analysis. (a) *hk*0 Diffraction Patterns. The diffraction pattern of sPP crystals (Figure 3a) is characterized by sharp spots along a^* at d spacings of 7.16 and 3.58 Å, indexed as 200 and 400, and consistent with the unit cell of Corradini et al.[2] However, the most distinctive and important feature of this diffraction pattern is the presence of an intense streak parallel to a^* at $b^* = (5.60\ \text{Å})^{-1}$; this streak is accompanied by reflections at 5.60 and 4.42 Å which are unequivocally indexed as 010 and 210. Neither the streak nor reflections with these spacings were observed in the fiber diffraction patterns of Corradini et al.[2] As a matter of fact, the space-group $C222_1$ selected in ref 2 *rules out* the existence of these reflections. We therefore investigated this matter in considerable detail and recorded a number of *hk*0 diffraction patterns from a variety of crystals. The *h*10 layers of some such patterns are seen in Figure 3b. They all show

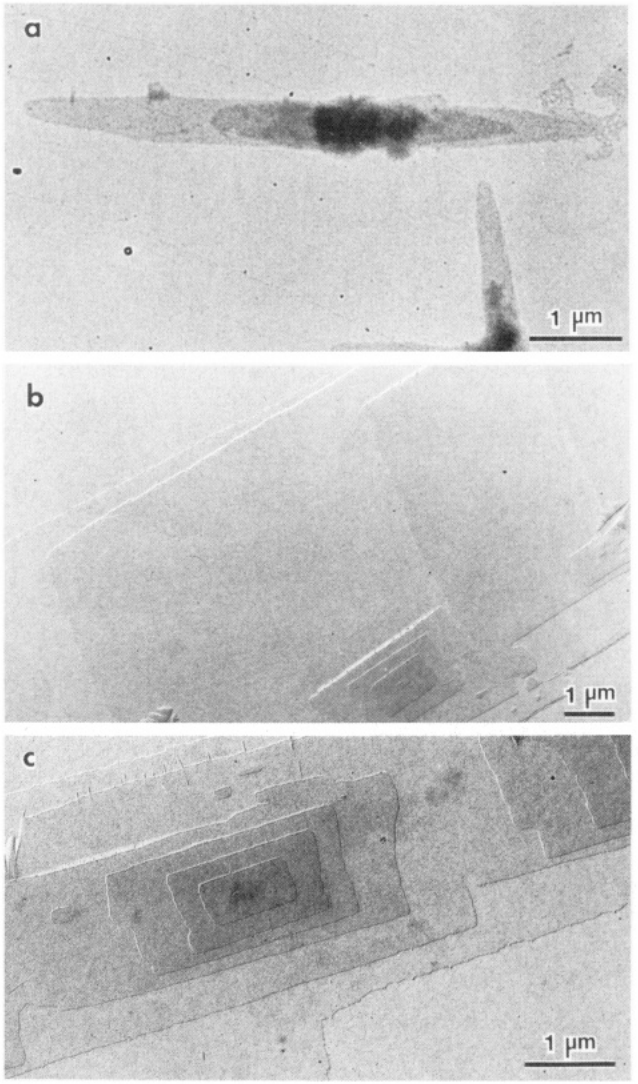

Figure 2. (a) Single crystal of sPP grown from 0.01% solution in toluene. (b and c) Single crystals of sPP grown from the melt in a thin film and seen at two different magnifications.

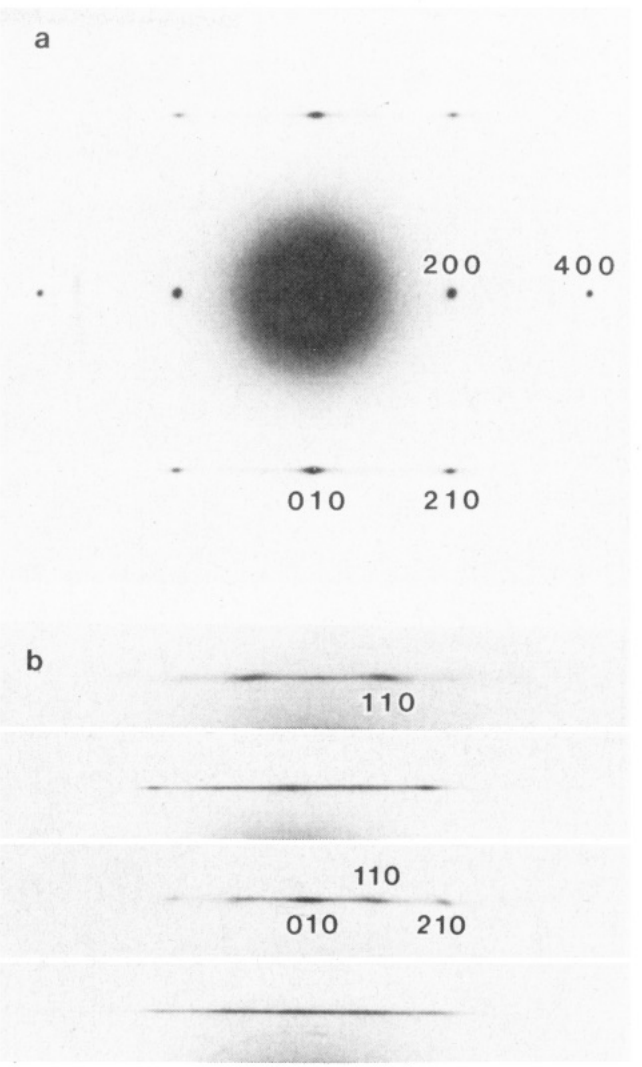

Figure 3. (a) Typical electron-diffraction pattern from single crystals of sPP, showing the characteristic streaking parallel to a^*. (b) Parts of electron-diffraction patterns from different sPP single crystals grown under the same conditions as in (a) and showing the variability in streaking.

quite systematically the streak, but they also display to varying extents either *three* reflections (at 5.60 and 4.42 Å, already indexed as 010 and 210), or *two* reflections, or all *five* reflections. The two additional reflections correspond to a spacing of 5.22 Å; they had been observed by Corradini et al.,[2] were indexed as 110, and are compatible with their proposed space group. Clearly, the crystals examined in our work consist of *two* structures (coexisting to varying degrees) that have very similar cell geometries and parameters but differ significantly in terms of the space group, i.e., in chain packing.

(b) *hkl* Reflections. In order to examine fully the three-dimensional lattice of sPP, we recorded electron-diffraction patterns from single crystals tilted about various axes. Four reciprocal-lattice sections of interest are shown in Figure 4. They correspond to rotation around the a axis by ±37° (Figure 4a) and ±56° (Figure 4b) and around the b axis by ±44° (Figure 4c) and ±60° (Figure 4d). A schematic diagram of the "reconstructed" reciprocal space and of the various sections is shown in Figure 5. Two features of the $hk1$ reciprocal plane are worthy of note: the sharpness of the $h11$ reflections and, more importantly, the existence of distinct streaks parallel to a^* with b^* coordinate of $\sim(11.20\ \text{Å})^{-1}$ (i.e., twice the corresponding value for the streak in the $hk0$ section). In Figure 4c, these streaks are intersected obliquely and thus appear as diffuse reflections; their real nature is better established in reciprocal-lattice sections parallel to a^* (Figure 4b). The streaks provide the only indication that the b axis repeat is *double* that originally considered, i.e., that the cell parameters are actually a = 14.50 Å, b = 11.20 Å, and c = 7.40 Å (albeit with a very strong subcell having b = 5.60 Å). For purposes of simplicity and consistency with previous work,[2] we will employ the smaller cell in this paper and will discuss the doubling of the cell only where necessary.

3. Intermolecular Packing. The above electron-diffraction evidence indicates that in the general case, the crystal structure of sPP is definitely related to that originally proposed by Corradini et al.[2] but may display significant differences in the packing of the chains. We now examine, after a short analysis of the previously proposed structure,[2] first those features that give rise to the streaking and to the new reflections in the $hk0$ plane and second those features that induce the doubling of the b axis.

(a) The Chain Conformation and the Structure of Corradini et al.[2] The $(t_2g_2)_2$ conformation of the sPP chain is equivalent to a helix with $s(2/1)2$ symmetry (see Figure 6a). A prominent feature is the trans position of successive CH_3 groups on both sides of the main-chain tt

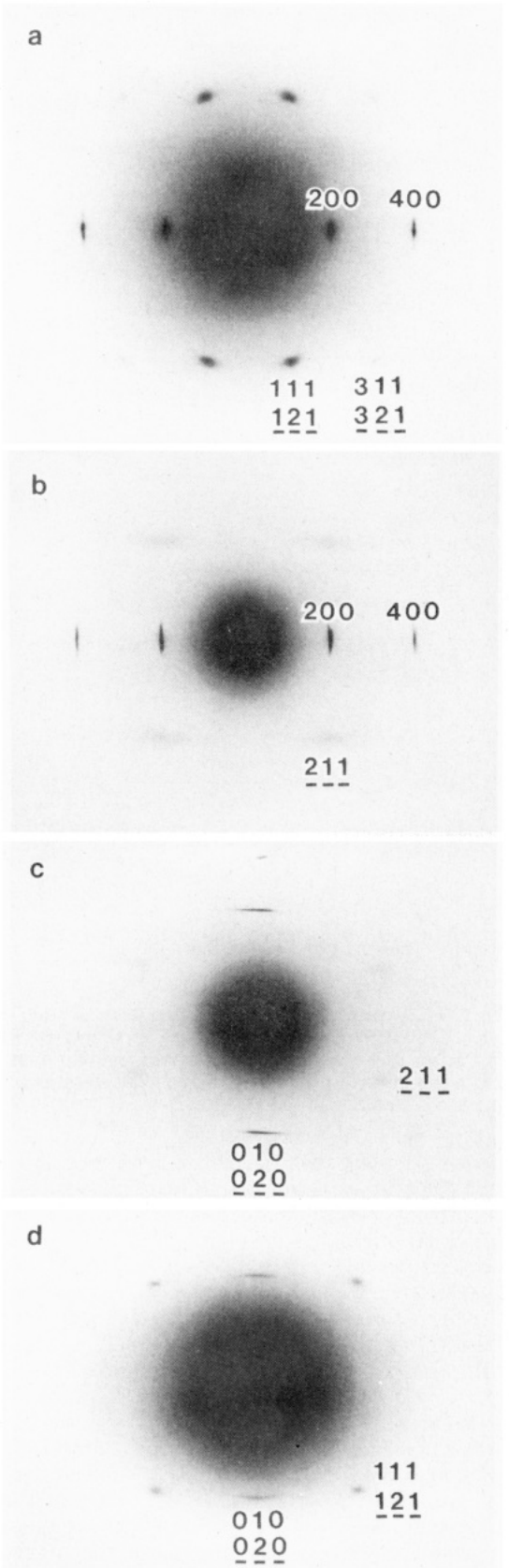

Figure 4. Electron-diffraction patterns from sPP obtained (as indicated also in Figure 5) by tilting (a) ±37° about *a*, (b) ±56° about *a*, (c) ±44° about *b*, and (d) ±60° about *b*. The indices shown are for the traditional unit cell with $b = 5.6$ Å and, when underlined, for the new cell with *b* doubled.

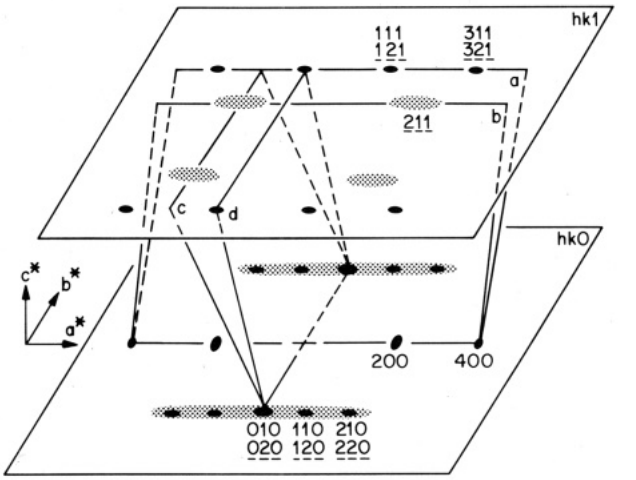

Figure 5. Schematic reconstruction of the reciprocal lattice of sPP showing the various planes examined in electron diffraction by tilting (a) ±37° about *a*, (b) ±56° about *a*, (c) ±44° about *b*, and (d) ±60° about *b*. The indices are given for the traditional unit cell having $b = 5.6$ Å and, when underlined, for the new cell for which *b* is doubled.

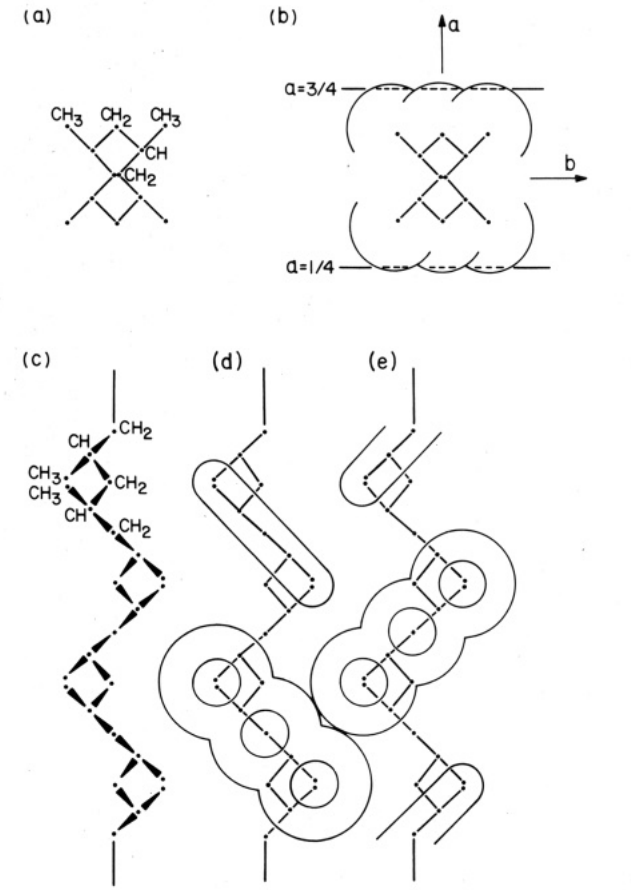

Figure 6. Molecular conformation of sPP as seen along the chain axis (a, b) or the *a* axis (c-e). The CH_2 and CH_3 groups are represented in (b) and parts of (d) and (e) as spheres with van der Waals radii of 2 Å. The caps of these spheres extending beyond the planes of intermolecular contact at $a = {}^1/_4$ and $a = {}^3/_4$ of (b) are shown in (d) and (e). Groupings of three such adjacent caps are drawn schematically as oblongs in the left- and right-handed sPP helices seen in (d) and (e), respectively.

groups. Therefore, the CH_3–CH–CH_2–CH–CH_3 sequences of sPP adopt the extended conformation of *n*-pentane; these segments lie on planes parallel to *bc* and make angles of ~45° with the chain axis.

In Figure 6b, the outer CH_3 and CH_2 groups are represented schematically by circular caps; these extend beyond the *bc* plane with coordinates $a = {}^1/_4$ or ${}^3/_4$, i.e., beyond the mean plane between two successive sheets. Schematic

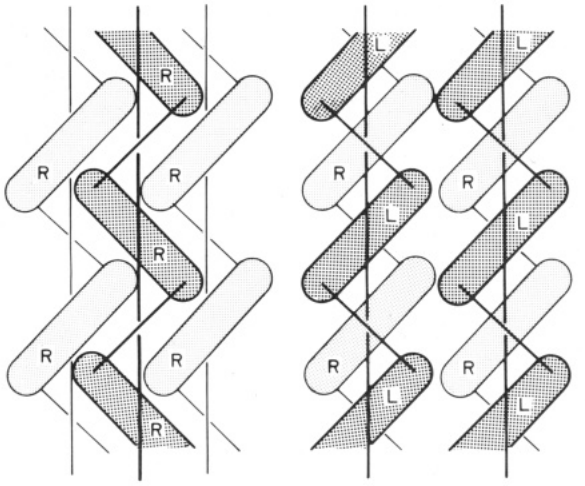

Figure 7. Possible intermolecular interactions in the planes with $a = {}^1/_4$ for various combinations of right- (R) and left- (L) handed helices. Groupings of three adjacent (CH_3, CH_2, CH_3) caps are shown as oblongs by using the schematic representation of Figure 6. Helices are seen on two adjacent sheets: those on the top sheet (helix axis at $a = 0$) are drawn in heavy lines, while those on the bottom sheet (helix axis at $a = {}^1/_2$) are drawn in light lines: (a) packing of sheets where all helices are of the same hand; (b) packing of sheets consisting of helices of opposite hand.

depictions of the front faces of left- and right-handed helices along the a axis are given in parts d and e of Figure 6, respectively.

The packing of these sheets leads, in the structure of Corradini et al.,[2] to a cell centered in the ab plane (cf. Figure 7a). The intersheet contacts are illustrated by using the representation of Figure 6d,e and are seen to be dominated by CH_3 and CH_2 contacts. As indicated by Corradini et al.,[2] this packing scheme results in methyl–methyl distances larger than 4.1 Å. When these are translated into contacts on planes with $a = {}^1/_4$ or ${}^3/_4$, they result in facile interdigitation of the CH_3 and CH_2 groups, which form the outer surfaces of the facing sheets.

(b) A Second Packing Mode of sPP Sheets. The aforementioned structure[2] implicitly assumes a *uniquely* specified helical conformation requiring either *all* left-handed helices or *all* right-handed ones. However, for a syndiotactic polymer, left- and right-handed helices are equally probable. If one considers the possibility of packing sheets composed of helices of *only one* hand, but with successive sheets containing helices of *opposite* hand, it is immediately apparent that the unit cell in this model is no longer centered in the ab plane. Rather, the chains in successive sheets *face* each other directly in c-axis projection and are displaced by $c/2$ in order to ensure interdigitation of the interacting CH_2 and CH_3 groups (Figure 7b).

From the above analysis of contacts between sheets, it appears that in principle the bc contact surface of any sheet offers *two* distinct packing possibilities to a newly depositing helix, depending upon the *hand* of the latter. If the hand is the same as that on the substrate sheet, the new helix will lie midway (along the a axis) between two substrate helices; if the hand is opposite, it will deposit itself directly in front of the substrate helices. In the light of the present analysis, the packing scheme observed by Corradini et al.[2] is only *one* of two possible limiting cases. All the $hk0$ diffraction evidence collected in the present work is linked to the existence of the *second* packing scheme, in either relatively pure form (thus giving rise to discrete 010 and 210 reflections at 5.60 and 4.22 Å) or

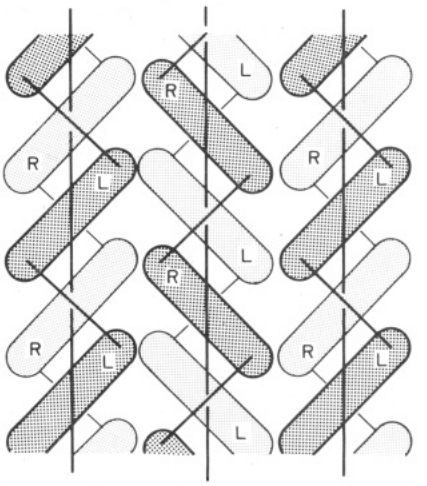

Figure 8. Same as Figure 7, but depicting packing of sheets each consisting of helices of alternating hand (RLR).

admixed with the first (thus resulting in the observed streaking of the reflections on the b^* row at 5.60 Å).

(c) Doubling of the Unit Cell. The above analysis of the packing of sheets is also based upon an assumption, namely, that *all* the chains in a given sheet have the same hand. The two resulting unit cells have different symmetry but the same dimensions (including specifically a b axis of 5.60 Å). However, neither of these two cells can account for our observed streaking on the first layer line at $(b^*)^{-1}$ = 11.20 Å, which suggests that the unit cell is *doubled* in the b-axis direction. The obvious origin of this streaking lies in the coexistence of helices of opposite hand within *individual* sheets. If this coexistence is in the form of a regular alternation of left- and right-handed helices within the same sheet, then an additional center of symmetry is introduced and the first-layer-line reflections should not be streaked. In any case, intermolecular contacts are comparable to those calculated for sheets made of helices of the same hand.

Coexistence of helices of different hand within single sheets may occur in a number of different ways, all of which have new and interesting consequences in terms of *intersheet* packing. Triad sequences of adjacent helices in the same sheet can be of the form RLR (equivalent to LRL), or RRL (equivalent to LRR, RLL, and LLR), or RRR (equivalent to LLL). A model of an RLR substrate is depicted schematically in Figure 8. Here, the arrangement of CH_3–CH–CH_2–CH–CH_3 sequences on the outer surfaces of the molecules is such that *only one* of the two aforementioned packing possibilities remains: The original[2] packing scheme giving rise to a centered cell is *ruled out* in this case and only that with chains directly facing each other in successive sheets is allowed (Figure 8). For an RRL substrate, there are two ways whereby molecules may be deposited (Figure 9): either (a) with consistently opposite hand, thus leading to the new packing scheme (Figure 9a), or (b) by incorporation of both packing modes, thus leading to a row vacancy of $b/2$ (Figure 9b). Which of these two possibilities is preferred will depend to a large extent upon growth regime, relative rates of adsorption of molecules of the same or opposite hand, as well as molecular-rewinding energetics. The final triad sequence to be considered (RRR) allows three possible packings: the two already discussed in relation to parts a and b of Figure 7 and the combined one incorporating a $b/2$ row vacancy similar to that of Figure 9b.

To summarize the various packing modes available to crystallizing molecules of sPP, we present in Figure 10 the

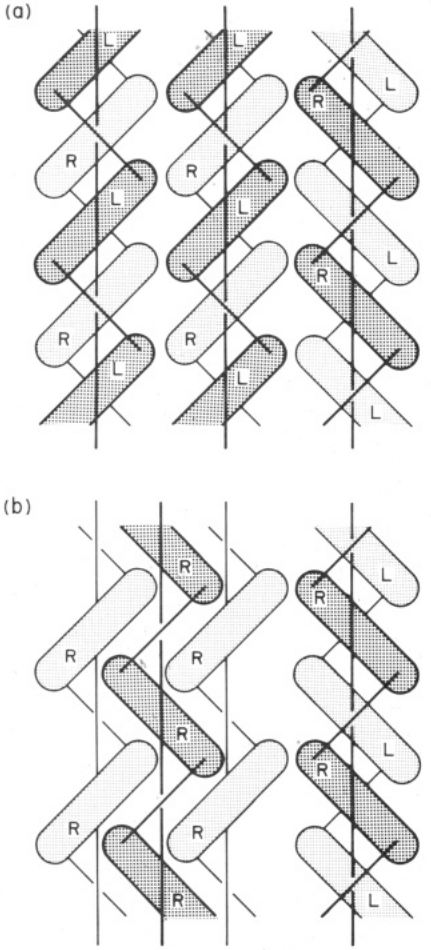

Figure 9. Same as Figure 8, but depicting two possible packing modes on substrate sheets of the RRL type: (a) with no vacancy; (b) with a $b/2$ row vacancy.

three simplest unit cells that result from *regularly* packed right-handed (R) and left-handed (L) chains, together with their corresponding $hk0$ diffraction patterns. Our observation of streaked and diffuse reflections implies departure from these regular lattices, in the form of mixed modes and row vacancies as described above.

(d) Space Group Analysis. The space group determined by Corradini et al.[2] ($C222_1$) is remarkable in that the full symmetry of the chain is maintained in the lattice, which makes it possible to use a single propylene residue as the crystallographic repeat unit although the conformational repeat unit is actually a dimer with conformation t_2g_2. With the dimer as the repeat unit, the symmetry would be reduced to $p2_12_12_1$. The alternative packing in which sheets of helices of one hand are deposited onto sheets of helices with opposite hand (Figures 7b and 10b) must be defined in terms of such a dimeric repeat unit and corresponds to the space group $Pca2_1$.

Quite interestingly, the structural repeat unit of the doubled cell (Figures 8 and 10c) is again reduced to a single residue. The corresponding space group is *Ibca*, with 16 monomeric units in the cell (as opposed to 8 for $C222_1$). The new lattice also maintains all the symmetry elements of the chain. The two space groups are closely related; the additional symmetry elements of *Ibca* reflect the regular alternation of left- and right-handed helices along the a and b axes.

Discussion

1. Crystal Structure and Growth Habit of sPP. We have provided in this work experimental evidence for

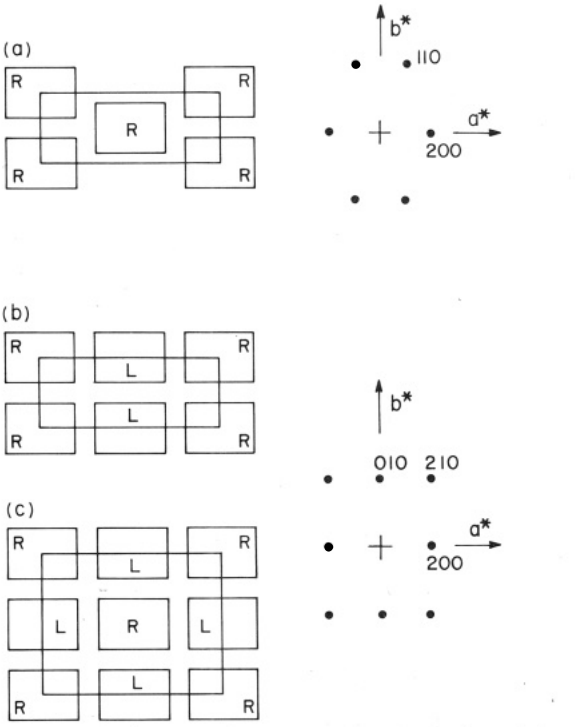

Figure 10. Unit cells of sPP (seen in c-axis projection) resulting from the three simplest regular modes of packing, together with their $hk0$ diffraction patterns: (a) all helices are of the same hand; (b) helices in adjacent sheets are of opposite hand; (c) helices in each sheet alternate in hand. The $hk0$ diffraction patterns of (b) and (c) are the same.

packing modes that are different from the C-centered lattice observed previously,[2] and we have explained these in terms of incorporation of helices of both hands. However, it is as yet not certain what underlies this newly found polymorphism of sPP. We do not attribute it to thin-film or substrate effects because we confirmed reflections of the new phase both in electron-diffraction patterns from thicker areas ($\sim$0.1 μm) and in X-ray diffractograms of bulk specimens. A second possibility is a mechanically induced structural transformation during orientation. At this point, we have not yet obtained highly oriented diffraction patterns from sPP, but films of low uniaxial orientation are consistent with our newly proposed structures. Moreover, since neither fiber patterns nor those from unoriented specimens were published in the original study,[2] a direct comparison is not available. A final possibility for the structural differences might be that crystalline structure and polymorphism are very sensitively coupled to *chemical* structure (e.g., degree of syndiotacticity, sequence distribution, blockiness) or to crystallization conditions; these possible effects are under investigation.

Irrespective of its origin, the crystalline polymorphism of sPP analyzed in this report is highly unusual in polymer crystallography insofar as it preserves both the chain conformation and the unit-cell geometry (neglecting for the moment our proposed b-axis doubling, which, as a consequence of the new packing mode, is discussed separately). Among polymers, the best known (if not the only) example of such preservation of both conformation *and* unit-cell dimensions across polymorphic forms is seen in poly(vinylidene fluoride), where the α- and the δ-phases differ solely in the type of interchain packing (antipolar vs polar, respectively[9,10]). On the other hand, this situation is not at all unusual among small organic molecules, for which optically active and racemic isomers often have the

same unit-cell geometry (including cell parameters) but a different packing of the molecules within the unit cell, i.e., a different space group. Quite expectedly, the space group of the racemic differs from that of the enantiomers by the presence of additional symmetry elements.

The molecular structure of syndiotactic polyolefins—and, for that matter, of isotactic polyolefins as well—offers the possibility for building helices that are related by a mirror symmetry and therefore for generating crystal structures based either on only one of the two possible helical conformations or on their mixture. Whereas the aforementioned behavior in small organic molecules has a *configurational* asymmetry at its root, in the present case the cause lies in a *conformational* asymmetry of helical macromolecules having *identical* configuration. We should also note that a comparable structure with one chain surrounded by four enantiomorphous chains has been reported[11] for the alternating copolymer of hexafluoroisobutylene and vinylidene fluoride, a semicrystalline polymer with physical properties similar to those of polytetrafluoroethylene. This polymer has a 2_1 helical chain conformation with an approximate t_2g_2 backbone similar to that of sPP. However, no crystalline polymorphism of the form reported here was observed in this copolymer.[11]

In terms of the morphology of sPP, several features of the relationship between structure and crystal habit should be underlined. The characteristic sheetlike intermolecular structure of sPP (already noted by Corradini et al.[2]) is certainly a contributing factor to its polymorphism and results in the observed behavior upon mechanical orientation (double orientation with distinct sheets parallel to *bc*).[2] The elongated habit of solution-grown sPP crystals is also in line with this structure (long axis parallel to *b*). However, when crystallized from the melt (in thin films), sPP exhibits marked *rectangular* crystal habits, which indicate growth on (100) as well as on (010) faces.

Growth of (100) faces, and, more specifically, nucleation of a new (100) layer has been stressed as the critical step in the observed phenomenon. For a substrate layer consisting of helices of a given hand, the *location* of the depositing chain depends upon the hand of the helix: either directly in front of the substrate helix (if of opposite hand), or halfway between two substrate helices (if of the same hand). As a consequence, the position of the growing layer is determined by the hand of the *first* depositing molecular stem! Moreover, in case of multiple nucleation (growth regime II), the growing layer may consist of various discontinuous portions that are displaced relative to each other by $b/2$: the positional uncertainty considered so far for successive (100) planes may equally well hold true within any given (100) plane. Molecularly resolved electron-microscopic images of crystals of sPP (as have been obtained with crystals of *n*-paraffins) would offer a potential means to observe experimentally the positional disorder associated with growth regime II.

Growth along (010) facets was considered by Marchetti and Martuscelli[4] as very unlikely, "the distance between two neighboring molecules being very large (14.50 Å)". With the new cell symmetry, the (010) plane becomes a *densely packed plane*, in fact the second densest (after (100)). It is therefore not surprising that the two clearly identifiable growth planes are (010) and (100) and that the resulting crystal habit tends toward rectangular: the observed growth habit and crystal symmetry are now fully consistent.

2. Structural Disorder in sPP and Lamellar Branching in iPP. When analyzed in molecular terms, the structural disorder in *syndiotactic* PP and the lamellar branching that characterizes the most common (α) phase of isotactic polypropylene[12-14] bear very strong resemblance. As a matter of fact, both of these phenomena are based on the helical hand of the molecular stem that initiates growth of a new layer; their morphological manifestations are, however, more distinct in iPP.

As discussed above, in sPP the hand of the depositing helix determines the crystallographic packing. Macroscopically, this phenomenon is not readily apparent, since it is seen only through the additional diffuse reflections and the streaking in diffraction patterns. On the other hand, in iPP the situation is morphologically so obvious that its origins had been under investigation for ca. 2 decades.[12-14] Here, the arrangement of 3_1 helices is such that the lateral (010) growth faces of the crystalline laths consist of helices of the *same* hand, which, however, alternates in successive (010) planes. Initiation of a new layer by a helix of opposite hand as that of the substrate results in the normal crystal lattice (there is no possibility of different packing modes in α-iPP). If, however, the helix is of the *same* hand as those on the substrate, it deposits epitaxially by rotation of $\sim 100°$ about the *b* axis, thus initiating growth of a "branched" lamella. Through continuous repetition, this growth scheme gives rise to the so-called "quadrites".

Even though these morphological manifestations of the coexistence of differently handed helices are much more pronounced in iPP, the frequency of branching in iPP is much smaller than the concentration of defects in sPP. This may result from the greatly different scale over which growth processes occur in iPP and sPP. In the isotactic polymer, the epitaxial deposition of a molecular stem ~ 100 Å long requires a crystallographically smooth (010) substrate of at least comparable lateral extent. On the other hand, the two different packing schemes in sPP result from the "localized" phenomena occurring at single stem sites and involving only small ($b/2$) lateral shifts of the depositing chain.

3. Configurational Character of sPP. The homogeneous syndiospecific polymerization of propylene results in a stereoblock sequence distribution. Zambelli and Allegra[16] have considered the polymerization mechanism in detail, and they propose a copolymerization model to account for the head-to-tail and tail-to-head propylene units, which involves primary and secondary monomer insertion by way of a four-center complex of pentacoordinated V^{III}. More recently, Corradini et al.[17] have put forward a new model for the origin of syndiotactic stereoregulation. Irrespective of the specific model chosen, the morphological regularity of our sPP crystals must be taken into account. Specifically, from electron micrographs such as in parts b and c of Figure 2, individual crystals of sPP consist of $\sim 10^{-16}$–10^{-17} g of material, i.e., of 10^2–10^3 chains having $\bar{M}_n \simeq 10^4$. These molecules are folded into lamellae 60–100 Å thick, which therefore implies stereoregular lengths of 30–50 monomer units (or somewhat less when the amorphous components at the surface are taken into account). Considering the imperfect syndiotacticity of our samples (76.9% racemic dyads), we must infer that, on the average, close to one quarter of the molecular content of these crystals is stereoirregular. Even if we assume a stereoblock distribution with preferential rejection of the nonsyndiotactic segments to the amorphous regions, it is still far from clear how such configurationally defective molecules yield such morphologically regular crystals extending to many micrometers in lateral dimensions (see particularly Figure 2b). Potential energy calculations for sPP lattices containing variable amounts of configurational

defects might be revealing in this regard.

Conclusions

Thin-film, bulk crystallization of sPP was shown to produce rectangular lamellar crystals with a unit-cell structure different from that originally proposed from doubly oriented samples. The new unit cell involves the presence of both left- and right-handed helices, consistent with the $(t_2g_2)_2$ conformation of sPP, whereas the existing unit cell was based implicitly upon helices of a *single* hand. In most crystals, the different packing schemes coexist, giving rise to a specific structural disorder of magnitude $b/2$. The two packing schemes depend upon the identical or opposite hand of crystallizing helices in relation to those on the crystal growth face. In addition, sheets on each (200) plane can also contain helices of opposite hand, which introduces a doubling of the b axis and necessitates the newly observed intersheet packing scheme.

Registry No. sPP, 26063-22-9.

References and Notes

(1) Permanent address: Institut Charles Sadron (CRM-EAHP), CNRS-ULP, 6, rue Boussingault, Strasbourg, France.
(2) Corradini, P.; Natta, G.; Ganis, P.; Temussi, P. A. *J. Polym. Sci., Part C* **1967**, *16*, 2477.
(3) Bunn, A.; Cudby, E. A.; Harris, R. K.; Packer, K. J.; Say, B. J. *J. Chem. Soc., Chem. Commun.* **1981**, 15.
(4) Marchetti, A.; Martuscelli, E. *J. Polym. Sci., Polym. Phys. Ed.* **1974**, *12*, 1649.
(5) Boor, J., Jr.; Youngman, E. A. *J. Polym. Sci., Polym. Chem. Ed.* **1966**, *4*, 1861.
(6) Boor, J., Jr.; *Ziegler-Natta Catalysts and Polymerizations*, Academic: New York, 1979; pp 117–122, 411.
(7) Zambelli, A.; Gatti, G. *Macromolecules* **1978**, *11*, 485.
(8) Schilling, F. C.; Tonelli, A. E. *Macromolecules* **1980**, *13*, 270.
(9) Bachmann, M. A.; Lando, J. B. *Macromolecules* **1981**, *14*, 40.
(10) Bachmann, M. A.; Gordon, W. L.; Weinhold, S.; Lando, J. B. *J. Appl. Phys.* **1980**, *51*, 5095.
(11) Weinhold, S.; Litt, M. H.; Lando, J. B. *J. Polym. Sci., Polym. Phys. Ed.* **1982**, *20*, 535.
(12) Lotz, B.; Wittman, J. C. *J. Polym. Sci., Polym. Phys. Ed.* **1986**, *24*, 1541.
(13) Khoury, F. *J. Res. Natl. Bur. Stand., Sect. A* **1966**, *70A*, 29.
(14) Padden, F. J., Jr.; Keith, H. D.; J. *Appl. Phys.* **1966**, *37*, 4013.
(15) Ogawa, T.; Elias, H.-G. *J. Macromol. Sci., Chem.* **1982**, *A17*, 727.
(16) Zambelli, A.; Allegra, G. *Macromolecules* **1980**, *13*, 42.
(17) Corradini, P.; Guerra, G.; Pucciariello, R. *Macromolecules* **1985**, *18*, 2030.

An Exact Method To Determine the Complete Orientation Distribution Function of the Chain Axis from an Arbitrary (*hkl*) Reflection†

Ravi F. Saraf

T. J. Watson Research Center, Yorktown Heights, New York 10598.
Received September 3, 1987; Revised Manuscript Received February 29, 1988

ABSTRACT: A pole inversion formula is derived for textures with an axis of symmetry, for example, planar and fiber orientation obtained by uniaxial and biaxial deformation processes, respectively. The measured pole density distribution function of an (*hkl*) reflection is expressed as an integral transform of the (required) pole density distribution function (which is usually the chain axis in polymers). Unlike other methods for pole inversion, this formulation does not involve any series expansion of the orientation functions. The integral equation is analytically solved for the special case when the (*hkl*) reflection is perpendicular to the chain axis, a common feature to most of the semicrystalline and liquid-crystalline polymers.

Introduction

The physical properties of (semicrystalline and amorphous) polymers, such as tensile modulus and strength, electrical and thermal conductivity, mass diffusion, and thermal expansivity, are dependent on chain orientation and extension. For semicrystalline polymers, a fraction of the chain (equal to the crystallinity) resides in the crystals, which are easier to orient compared to the amorphous phase. The changes in physical properties are thus dependent on the overall crystal texture. One method to tailor the crystal texture for improving a particular property in a given direction is by deformation. For example, by uniaxial extension, the tensile modulus is enhanced by 100-fold in polyethylene and[1,2] electrical conductivity is improved by 10-fold in polyacetylene at a draw ratio of ~ 3.[3] Thermal conductivity increases by 30-fold on drawing polyethylene by 32×,[4] and diffusivity of toluene in polypropylene drops by 30-fold at a draw ratio of 18.[5] However, the properties in the orthogonal directions are inferior to those in the initial, undeformed sample. A more "uniform" enhancement of properties (with some sacrifice of highest possible property enhancement) can be attained by more complex deformation geometries, such as biaxial stretching,[6-11] uniaxial compression,[12,13] planar deformation,[14,15] and combinations of various deformation geometries.[16-18]

Wide-angle X-ray diffraction (WAXD) is a suitable method for crystal texture analysis of polymers obtained by the above-mentioned deformation geometries.[19-22] The crystal texture is expressed in the form of a "pole figure". Pole figure plots represent the orientation distribution of a given (*hkl*) reflection with respect to the lab-frame. For isotropic orientation, the tip of the $\mathbf{R}(hkl)$ vector (perpendicular to the (*hkl*) plane) scribes a uniform orientation density sphere. For anisotropic orientation, a nonuniform orientation density is expected. The orientation density distribution on the sphere is represented by three projections along three orthogonal directions (usually the lab-frame axes). These three projections of the orientation sphere are called the pole figures. The tip of the $\mathbf{R}(hkl)$ vector is called the pole of the (*hkl*) reflection on the orientation sphere, and the orientation distribution is also called the pole density. Thus, for isotropic sample, the pole density is constant on the orientation sphere for any (*hkl*) reflection.

To relate the crystal texture to the modified anisotropic property, the orientation distribution of the chain axis (which is usually labeled as the c-axis in the crystal) is the

† Dedicated to Prof. Roger Porter on the occasion of his 60th birthday.

0024-9297/88/2221-2382$01.50/0